Particle size segregation in two-dimensional circular granular aggregates

Jérémy Sautel, Charles-Édouard Lecomte, and Nicolas Taberlet*
Université Lyon, ENS de Lyon, Université Claude Bernard, CNRS, Laboratoire de Physique UMR 5672, F-69342 Lyon, France

(Received 18 December 2020; accepted 14 January 2021; published 9 February 2021)

Although many previous studies have focused on the Brazil nut effect, segregation in a self-gravitating circular aggregate remains relatively unexplored. In this paper, size segregation in a two-dimensional assembly of grains in a circular geometry is studied through discrete element method (DEM) numerical simulations. We show that radial segregation within an asteroid submitted to periodic perturbations is not limited to the surface but also occurs in its core. The characteristic time and the overall efficiency of the segregation mechanism are studied as the intensity of the perturbation, the frictional properties, and rotational freedom of individual grains are varied.

DOI: 10.1103/PhysRevE.103.022901

I. INTRODUCTION

In the last decade, the space missions Hayabusa and, more recently, Hayabusa 2 have focused on so-called rubble-pile asteroids which consist of a loose assembly of dry grains held together by their mutual (weak) gravitational attraction [1,2]. The OSIRIS-REx mission is currently going on to study asteroid (101955) Bennu [3] and has already lead to interesting results about its surface properties by imaging and thermal analysis [4]. In October 2020, it successfully collected a sample of asteroid (101955) Bennu, and its arrival on Earth for analysis is expected in 2023. These past and current missions show a strong interest by the scientific community in rubble-pile asteroids, and significantly increase our knowledge of these small bodies. As a consequence, they have piqued interest of the granular matter community as well.

Although many asteroids have a monolithic nature, rubble-pile asteroids consist of a granular aggregate, at least in a surface layer [5]. Concerning their cores, no exploration has been done yet, and their nature and composition remain not well known. However, some studies have addressed the problem of their core constitution by using the external mechanics and cohesion properties of the aggregates [6]. The best known examples of these rubble-pile asteroids are asteroids (25143) Itokawa, (162173) Ryugu, and also Bennu which is currently under study by the OSIRIS-REx mission. These are of particular interest because their surfaces, especially that of Itokawa, show a strong presence of large boulders, reaching one tenth of the asteroid typical size. This concentration of the largest components of the granular medium at its surface, with respect to local gravity, suggests that a particle-size segregation phenomenon might occur in the asteroid [7]. Rubble-pile asteroids are not immutable and can rearrange due to a number of phenomena. They may undergo collisions with a smaller body, be submitted to tidal forces near larger objects, or experience an increase in spin rate due to the solar radiation pressure, known as the YORP (Yarkovsky-O'Keefe-Radzievskii- Paddack) effect [8,9]. For all these reasons, the eventuality of a segregation process on asteroids requires further examination. This can reasonably be done by using numerical experiments, as they enable one to easily control all the relevant physical parameters of the aggregate. The results of the corresponding simulations bring a lot of information about the mechanics of segregation in this original geometry. Moreover, they are of great help to establish predictions about the granular composition of the aggregate below the surface of the asteroid, as this information is not accessible through direct measurements yet.

Previous numerical studies have focused on granular segregation in asteroids. Maurel *et al.* [10] have simulated the dynamics of a large intruder inside a granular bed, under vertical vibration and in a low gravity field. Although they show that friction plays an important role into this problem, the geometry used in this study hardly applies to asteroids, as the perturbation is nonisotropic. Perera *et al.* [11] simulated a spherical granular aggregate and observed an incomplete size segregation, as the core of the aggregate remained mixed after several perturbations. This may be due to the number of grains implemented (a few hundred), which may be low for a three-dimensional (3D) aggregate. A segregation mechanism was also proposed by Shinbrot *et al.* [7]: They suggest a differential accretion of smaller grains, whether they collide on a large grain or on a group of small grains.

Granular segregation mechanisms have been studied in the terrestrial environment, both experimentally [12–14] and numerically [15]. Although the granular medium was often vertically vibrated, the influence of horizontal vibration [16] and the case of a rotating drum [17] have also been investigated. All these studies highlighted the roles of convection [14], percolation, and rearrangements [18,19] in the size segregation process, commonly named the "Brazil nut effect."

In this paper we propose to show that the classical results from the granular physics literature can reproduce the observations made on rubble-pile asteroids. To this aim, we present results from numerical simulations of an assembly

*nicolas.taberlet@ens-lyon.fr

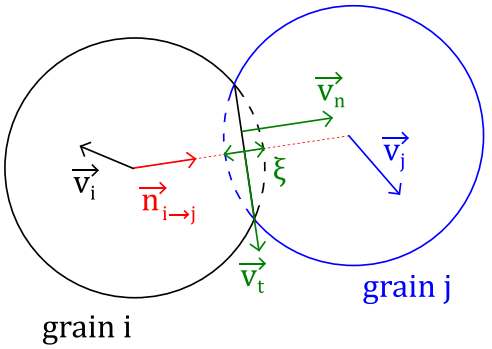

FIG. 1. Two grains in contact: Illustration of the overlap and relative speeds in the simplified case where the grains have no rotational motion.

of grains (submitted to a central gravitational force) which undergoes regular mechanical taps (see details in Sec. II). Our simulations therefore aim at extending the classical Brazil nut segregation results (in a uniform gravitational field) to a circular (and spherical) geometry, with a nonuniform gravity (both in intensity and direction). The paper is organized as follows. The numerical methods are described in Sec. II. In Sec. III quantities that help quantify the segregation dynamics are defined. Section IV presents the effect of physical parameters, among which are the intergrain friction coefficient, the inelasticity of the collisions, and the intensity of the periodic perturbations.

II. NUMERICAL METHODS

In the present paper, the asteroid is modeled using a largely simplified system, which consists of a 2D assembly of disks (see Fig. 2). Individual grains are free to rotate and the forces and torques acting on each individual grain are determined using Newton's laws in order to compute their position, speed, and rotation speed in a time-driven simulation scheme, using a soft-spheres discrete element method (SSDEM) [20].

The gravitational field within the asteroid pulls each grain toward the overall center of mass, and is assumed to remain linear, which corresponds to a round asteroid. Therefore, the only interactions that exist between the grains are frictional history-dependent contact forces [21]. In order to mimic the well-known segregation experiments in which a container is submitted to periodic taps on its bottom, the gravitational field is reversed for a short time period, which briefly pushes the grains away from the center, causing the asteroid to dilate (by up to 5%). In the following, this will be referred to as a quake. Let T be the period and T_S the duration of a perturbation ($T_S < T$). During each interval of time $[NT, NT + T_S]$ (N being an integer $\geqslant 1$), the imposed gravitational field is reversed, meaning that the grains are suddenly pushed outwards. This lasts for a short time T_S, before the grains collapse to form the aggregate again. The duration of this phase allows one to control the intensity of the perturbation. The period $T = 12.5$ s is chosen so that the grains have come to a complete rest before experiencing the next quake.

Note that the radial expansion induces no shear since the medium is freely expandable, as individual grains can easily detach from one another. Again, it should be noted that this procedure is not intended to mimic any actual source of

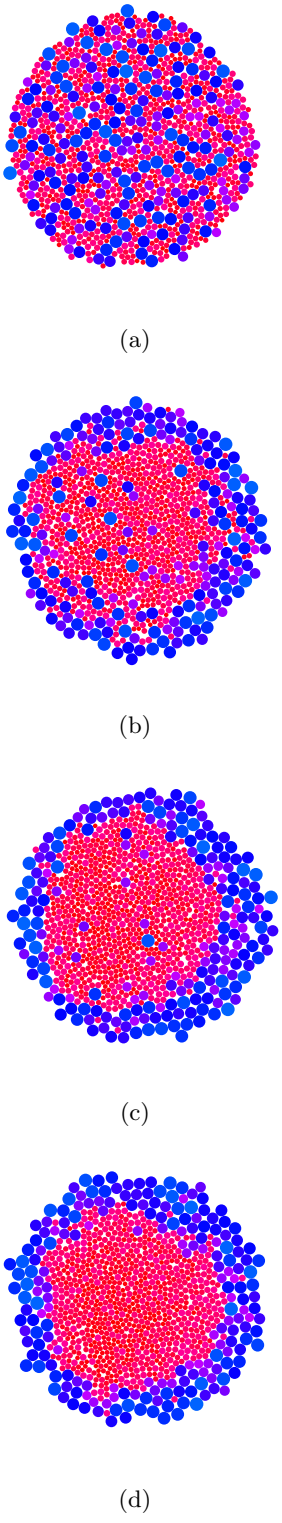

FIG. 2. Snapshots of a simulated aggregate at different times. (a) Initial state. (b) After 500 quakes. (c) After 1000 quakes. (d) After 2000 quakes. The color of the grains depends on their size, globally resulting in blue large grains and red small grains. These data were obtained for a friction coefficient $\mu = 0.8$, a perturbation duration $T_S = 1.25$ s, and a dimensionless momentum of inertia $J^* = 10^4$ (meaning that the rotation is largely hindered).

rearrangements in actual asteroids, but should be seen as a controlled isotropic perturbation.

The granular medium is composed of two main populations of grains: The "large grains" (radii $R_i \in [0.8, 1.2]$) and the "small grains" $R_i \in [0.4, 0.6]$, both distributions being uniform. The $\pm 20\%$ polydispersity is intended to avoid crystallization. These distributions are of course much simpler than the one measured on granular asteroids surfaces [22,23], but they enable simple simulations and already lead to a good understanding of segregation in asteroid-like aggregates. A total number of 1000 grains is implemented: 200 large grains and 800 small grains, ensuring that both populations cover the same area.

The two-dimensional model of an asteroid is obtained by first placing 1000 grains on a series of circular rings of center O. This point is also chosen as the center of mass of the asteroid. Rather than computing each gravitational interaction between all grains, each grain is submitted to a central force directed towards O, proportional to its mass m_i and distance to O. It is thus intuitive to work in the polar coordinates associated with O. Denoting as M_i the location of a given grain i, $r_i = OM_i$, the central force $\overrightarrow{F_i}$ applied to this grain reads:

$$\overrightarrow{F_i} = -m_i g \frac{r_i}{R_{\text{ast}}} \hat{\mathbf{r}}. \tag{1}$$

where R_{ast} is the estimated radius of the circular 2D asteroid once all the grains have collapsed and g is the surface gravity of the asteroid. The expression of $\overrightarrow{F_i}$ is obviously inspired by the gravitational field inside a self-gravitating body. Imposing this central force on each grain instead of computing the gravitational forces between all the grains results in a strong improvement of the simulation's efficiency.

In the present paper, the overall radius of the asteroid is kept constant but its influence on the segregation process would certainly deserve further investigation. Note, however, that even for large values of R_{ast} the system would differ from the standard tapping problem since the gravitational field is never uniform in our study.

When in contact, two grains i and j apply on each other both a normal force and a history-dependent tangential friction force (see Fig. 1). In this study, for the normal force a linear-dashpot model [24,25] with a stiffness constant $k_n = 10^4$ N m^{-1} and a damping constant $\gamma = 30$ kg s^{-1} is used. Moreover, the tangential displacement $\overrightarrow{\delta_t}(t)$ of i with respect to j is computed. This displacement is integrated over all the duration of the contact. The friction coefficient between the grains is μ. We use the Cundall model [21] to compute the tangential contact force: At a given time t, $k_t||\overrightarrow{\delta_t}(t)||$ is compared to $\mu||\overrightarrow{F_N}(t)||$. If $k_t||\overrightarrow{\delta_t}(t)|| < \mu||\overrightarrow{F_N}(t)||$, the contact is not sliding and the tangential force behaves as a linear spring: $\overrightarrow{F_T} = -k_t\overrightarrow{\delta_t(t)}$, with $k_t = 2k_n/7$ [20,21]. In contrast, if $k_t||\overrightarrow{\delta_t}(t)|| \geqslant \mu||\overrightarrow{F_N}(t)||$, then we consider a sliding contact with $||\overrightarrow{F_T}|| = \mu||\overrightarrow{F_N}||$. To summarize, the norm F_T of the tangential force is given by

$$F_T = \max[k_t\delta_t(t), \mu F_N(t)]. \tag{2}$$

This models the Amontons-Coulomb laws of solid friction.

A standard radius $R^* = 1$ and a standard mass $m^* = 1$ are defined. The mass of grain i is given by $m_i = m^*(R_i/R^*)^2$ and its moment of inertia is $J_i = J^* m_i R_i^2/2$. Note that m^* (kept constant) implements the density of the grains, and the introduction of J^* (variable) enables us to artificially increase the moment of inertia, in order to reduce the rotational moment of the grains.

From the normal and tangential forces of each contact, the resulting force and torque applied on each grain are computed at time t, and Newton's laws are numerically integrated using the Verlet algorithm in order to simultaneously compute all new positions of the grains at time $t + dt$. The time increment value is fixed at $dt = 5 \times 10^{-4}$ s, such that $\mathrm{d}t \ll \sqrt{m/k}$ for every grain, entailing a reasonable description of the contacts.

III. DEFINITION OF SEGREGATION CHARACTERISTICS

In order to quantify the segregation in a given aggregate, one can define a segregation degree based on the positions of individual grains. As a reminder, R_i denotes the radius and $r_i = OM_i$ the position of grain i. The segregation degree ψ is defined, at any time, as

$$\psi = \frac{\langle r_{\text{large}} \rangle}{\langle r_{\text{all}} \rangle} = \frac{\sum_{i\in\text{large}} {R_i}^2 r_i \big/ \sum_{i\in\text{large}} {R_i}^2}{\sum_{i\in\text{all}} {R_i}^2 r_i \big/ \sum_{i\in\text{all}} {R_i}^2}. \tag{3}$$

This means that the distances to the center O are weighed by the surface area of the grains. This is justified, as the physical meaning of $\langle r_{\text{large}} \rangle$ is the average distance to O of the area covered by the large grains. Note that, in a completely mixed state, this average distance is the same for all the grains and thus the segregation degree takes the value $\psi = 1$. A completely segregated state would be obtained if all the small grains were resting in a disk of radius R_s and all the large grains resting in a ring between R_s and the radius of the asteroid R_{ast}; the bottom panel of Fig. 2 gives a good illustration of this kind of state. If α_A is the area fraction that is covered by the large grains, then $R_s = \sqrt{1-\alpha_A} R_{\text{ast}}$. By approximating the aggregate with a continuous medium, one can evaluate $\langle r_{\text{large}} \rangle$ and $\langle r_{\text{all}} \rangle$, which leads to a maximum value $\psi_{\max} = \frac{1-(1-\alpha_A)^{3/2}}{\alpha_A}$.

It is simpler to use a segregation degree which ranges from 0 for a perfectly mixed state to 1 for a completely segregated state, as one can define a normalized segregation degree:

$$\Psi = \frac{\psi - 1}{\psi_{\max} - 1}. \tag{4}$$

A typical evolution of Ψ is shown by Fig. 3.

Four snapshots of the corresponding asteroid are displayed in Fig. 2 and show a very clear size segregation. After 500 quakes, the segregation is not complete but after 2000 there remains no large grain in the core of the simulated asteroid. The evolution of the corresponding segregation degree Ψ is given in Fig. 3. The initial state is perfectly mixed ($\Psi \simeq 0$) while the asteroid is entirely segregated after 2000 quakes ($\Psi \lesssim 1$). Note that the segregation occurs after the first few quakes with no delay, and slowly tends towards a steady state at longer times. The use of an exponential fitting curve $\Psi(t) = \Psi_\infty[1 - \exp(-\frac{t}{\tau})]$ to fit $\Psi(t)$ enables one to define two characteristic quantities: The steady segregation

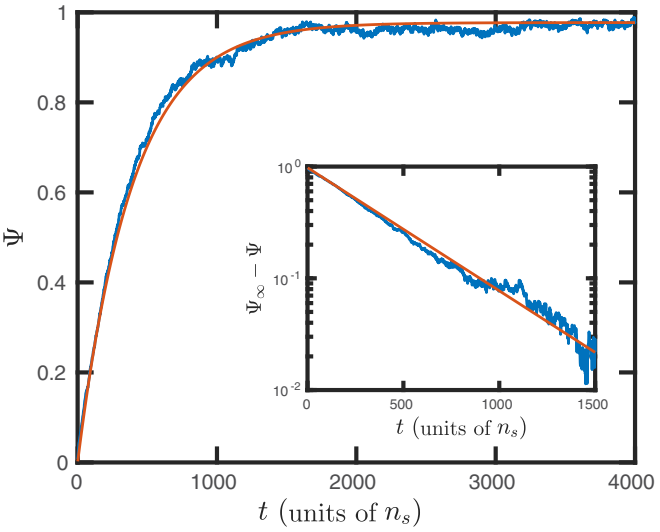

FIG. 3. Plot of the segregation degree Ψ as a function of time (in number of quakes), computed for $\mu = 0.8$, $T_S = 1.25$ s, and $J^* = 10^4$, corresponding to the aggregate shown in Fig. 2. The red curve corresponds to an exponential fit: $\Psi(t) = \Psi_\infty[1 - \exp(-\frac{t}{\tau})]$. The inset is a semilogarithmic plot of $\Psi_\infty - \Psi$ in for the same data and fit.

degree, Ψ_∞, and the characteristic segregation time, τ. It should be emphasized that the exponential law is not derived from any theoretical considerations but is only a simple mathematical function used to fit the data. The evolution of Ψ_∞ and τ with the different physical parameters of the aggregate is therefore a useful tool to study the segregation mechanism.

IV. INFLUENCE OF THE PHYSICAL PARAMETERS

A. Strength and intensity of the perturbation

As described above, the quakes that are applied to the asteroid consist of an inversion of the central gravitational field during a time interval T_S, which therefore sets the intensity of the perturbation.

We investigate the influence of the perturbation's strength by varying T_S below or above the standard value $T_S = T/10 = 1.25$ s. However, the time T_S is not the only parameter that affects the strength of the perturbations. Indeed, the surface gravity g that is imposed also plays an important role, due to the fact that inverting the gravitational field during a fixed time T_S will result in larger displacements of the grains if g is larger. The energy injected into the system per quake is given by $E = 3/2\, M_{\text{ast}}\, g\, R_{\text{ast}} \sinh^2(T_s\sqrt{g/R_{\text{ast}}})$, where $M_{\text{ast}} = \Sigma\, m_i$ is the overall mass of the asteroid. $T_s\sqrt{g}$ therefore appears as a relevant parameter, but plotting Ψ_∞ and τ as functions of $Ts\sqrt{g}$ (as in Fig. 4) is not expected to lead to a collapse on a master curve. The investigated values range from $T_S = 1$ s to $T_S = 1.75$ s. For each value of T_S, three different values of friction coefficient were used (except when $g \neq 1$, in which case only $\mu = 0.5$ is plotted). The explored values of g and T_S are never large enough to permit percolation of the small grains between the large ones, as two neighboring large grains are never pulled far enough from each other to let a small grain pass. Consequently, only local rearrangements can occur.

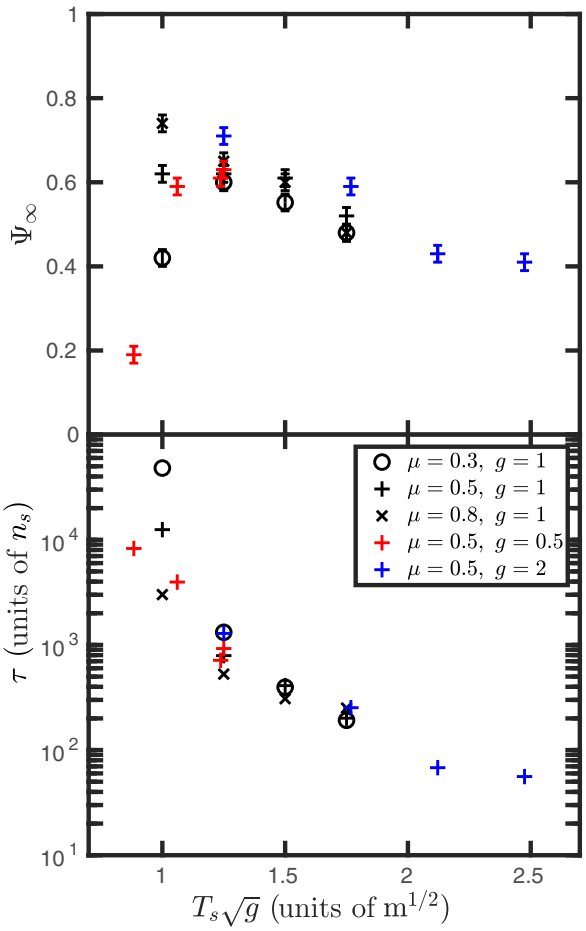

FIG. 4. Plot of Ψ_∞ (top) and τ (bottom) as functions of the perturbation strength $T_S\sqrt{g}$ with g ranging from 0.5 to 2, and μ from 0.3 to 0.8 (details in the legend). We note a monotonic decrease of τ as the perturbation becomes stronger. In contrast, the quality of the segregation reaches an optimal value for a given strength.

In particular, we notice a monotonic decrease of τ as the perturbation strength increases. This decrease is very strong, as τ vanishes by almost 3 orders of magnitude when $T_S\sqrt{g}$ only increases by a factor 2.5. Stronger perturbations enable larger movements during the perturbation, which lead to more rearrangement when the aggregate collapses again at the end of the perturbation. As these rearrangements are the main source of segregation in our study, we conclude that this will cause an acceleration of the segregation process. Considering the quality of the segregation Ψ_∞, we observe an optimum for each value of μ. For $\mu = 0.8$, this optimum is above 0.7 and is reached for $T_S\sqrt{g} = 1\ m^{1/2}$. For $\mu = 0.3$ and $\mu = 0.5$, the optimum is reached for $T_S\sqrt{g} = 1.25\ m^{1/2}$ and $T_S\sqrt{g} = 1\ m^{1/2}$ respectively. This is also explained by the rearrangement mechanism: If there is no perturbation ($T_S\sqrt{g} = 0\ m^{1/2}$), there will be no rearrangement and no segregation will happen. Then, as one increases $T_S\sqrt{g}$, rearrangements will happen and naturally lead to a segregation. However, if one increases $T_S\sqrt{g}$ too much, the perturbation will be too strong for the system to reach a steady segregated pattern.

B. Friction coefficient

The friction coefficient μ is expected to play a role in the segregation process. Indeed, the rearrangements of the grains after each perturbation are the source of segregation in our simulations. These rearrangements involve a large number of contacts between the grains, and the associated friction forces certainly have a strong influence on the mechanical state in which the aggregate stabilizes after a perturbation. To investigate this effect, and to emphasize the essential role of the rearrangements, we propose to study the mean absolute displacement of individual grains between two consecutive quakes. This absolute value, $\overline{d}$, is the displacement in the 2D space, taking into account both radial and azimuthal movements. The value of $\overline{d}$ is then averaged over the τ first perturbations. We also compute the mean displacement $\overline{d_s}$ taking into account the small grains only, and $\overline{d_l}$ with the large grains only. Figure 5 shows the evolution of this mean displacement $\overline{d}$ as a function of μ, for different values of T_S and $g = 1$.

Two main observations can be made. First, a minimum in mean displacement appears for each value of T_S.

The corresponding value $\mu_{\min}$ seems to increase slightly with T_S, and to remain in the range [0.2, 0.4] for the explored range of T_S. Second, we obtain $\overline{d_s} \geqslant \overline{d_l}$ for $\mu \leqslant \mu_{\min}$ and $\overline{d_s} \leqslant \overline{d_l}$ for $\mu \geqslant \mu_{\min}$ (except for the lowest value $T_S = 1$ s, for which we observe $\overline{d_s} \geqslant \overline{d_l}$ in the complete range of μ). This means that when the friction coefficient is smaller than $\mu_{\min}$, the small grains are more mobile whereas the large grains become more mobile for a friction coefficient greater than $\mu_{\min}$. Physically, and from the observations that were made regarding the strength of the perturbation, one expects that the more the grains move during one perturbation, the faster the segregation is. Mathematically, one expects τ to be a decreasing function of $\overline{d}$. Figure 6 is a plot of τ as a function of $1/\overline{d}$, which shows a dramatic growth of three orders of magnitude for $1/\overline{d}$ increasing in the range [0,30]. Thus, our results confirm the interpretations in terms of rearrangements made in the study of the perturbation strength.

Concerning the quality of the segregation, one can observe a clear correlation between Ψ_∞ and the difference of mobility between the large and the small grains, quantified by $\overline{d_l} - \overline{d_s}$. The evolution of Ψ_∞ as a function of $\overline{d_l} - \overline{d_s}$ is plotted in Fig. 7, which shows a clear increase in Ψ_∞ with increasing $\overline{d_l} - \overline{d_s}$. Note that for the highest perturbation intensity ($T_S = 1.75$ s) the segregation quality is lower. This corresponds to the previous observation that at high T_S it is more difficult to reach a segregated steady state of good quality. In contrast, one can notice a high quality segregation for the simulations with an artificially increased moment of inertia of the grains. The study of this parameter is the topic of the next section.

C. Moment of inertia

The observation that there exists a friction coefficient $\mu_{\min}$ for which the mean displacement of the grains reaches a minimum appears nonintuitive. To elucidate this fact the fraction α_S of grain-grain contacts that are in a sliding regime is computed. Figure 8 shows that α_S is a decreasing function of μ which can be empirically fitted by $\alpha_S(\mu) = 1 - \mu/\mu_0$,

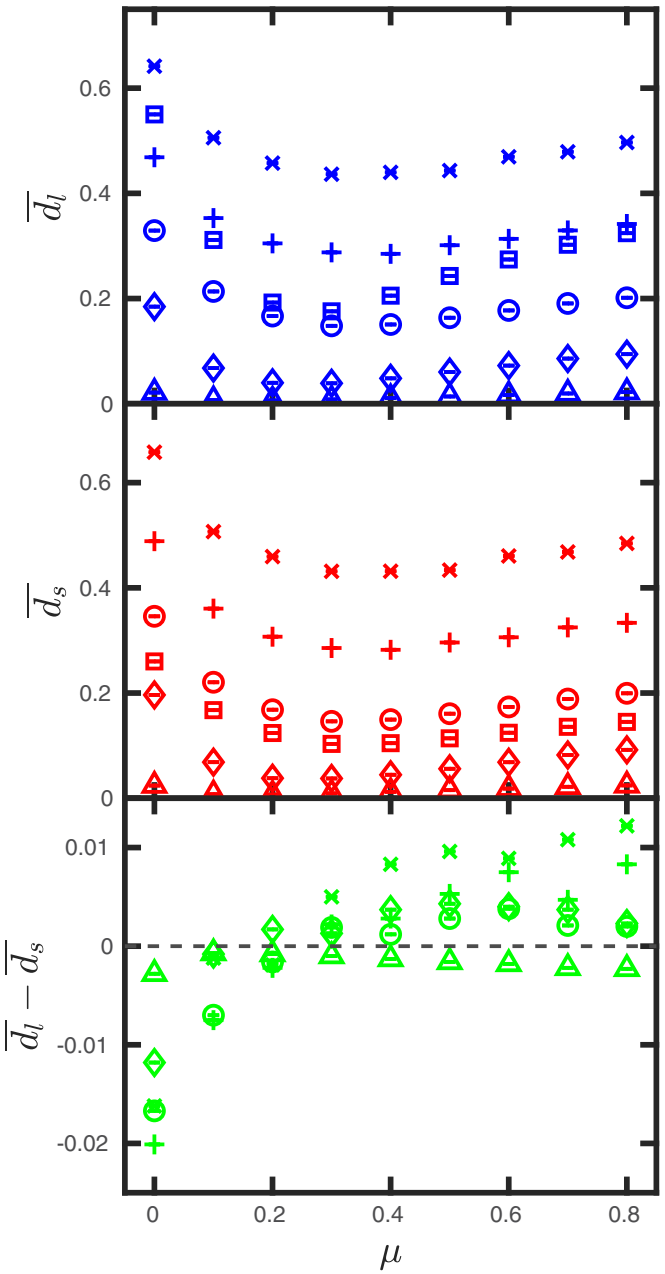

FIG. 5. Plot of the mean displacements: $\overline{d_l}$ computed over the large grains only (top, blue), $\overline{d_s}$ computed over the small grains only (middle, red), and the difference $\overline{d_l} - \overline{d_s}$ (bottom, green) as functions of the friction coefficient, μ. △: $T_S = 0.5$ s; ◇: $T_S = 1$ s; ○: $T_S = 1.25$ s; +: $T_S = 1.5$ s; ×: $T_S = 1.75$ s. The □ correspond to the mean displacements for monodisperse aggregates containing large grains only (top, blue) or small grains only (middle, red), with $T_S = 1.25$ s.

at least in the range $\mu \in [0, 1]$, with $\mu_0 \simeq 1.3$. This is more intuitive: Indeed, in the nonfrictional case all contacts are sliding, but the more friction there is, the more difficult it is for individual contacts to enter the sliding regime. For each individual sliding contact the tangential force is given by $F_T = \mu F_N$, where F_N is the normal force, while, for a nonsliding contact, $0 \leqslant F_T < \mu F_N$. As an assumption, one can consider in the latter case that, on average, $\overline{F_T} = \frac{1}{2}\,\mu\overline{F_N}$. Given these aspects and (2), we deduce that the average tangential force

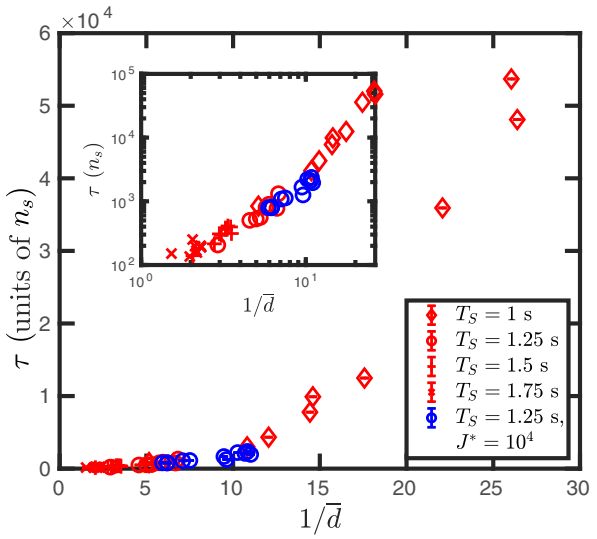

FIG. 6. Plot of the segregation time τ as a function of the mean displacement. The red ticks correspond to the different values of T_S. The blue ticks correspond to different values of the moment of inertia of the grains, which are discussed in Sec. IV C. The inset is a plot of the same data on a log-log scale.

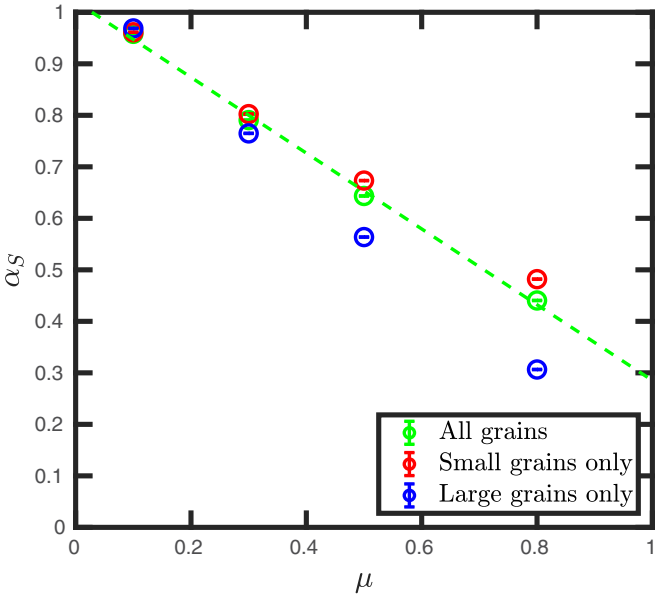

FIG. 8. Plot of the fraction α_S of contacts in the sliding regime as a function of the friction coefficient μ. The fraction α_S decreases linearly with μ in the explored range.

$\overline{F_T}$ between two grains reads

$$\overline{F_T} = \alpha_S \mu \overline{F_N} + (1-\alpha_S)\mu \frac{\overline{F_N}}{2} = \frac{\overline{F_N}}{2}\mu\left(2 - \frac{\mu}{\mu_0}\right). \quad (5)$$

Given this expression, it appears that there is a value of μ that maximizes the average tangential force in one grain-grain contact, and consequently minimizes the mean displacement of one grain between two consecutive quakes. This explains the observation of a value $\mu_{\min}$, but it predicts $\mu_{\min} \simeq 1.3$. However, this predicted value is larger than the one observed in Fig. 5 ($\mu_{\min} \simeq 0.3$). The difference may come from the fact that the tangential force not only reduces the translational motion of the grains, but it also produces a rotational motion of the grains. To investigate the specific effects of μ on the translational and rotational degrees of freedom of the grains, their moment of inertia was artificially modified (while all other parameters were kept constant). As a reminder, the moment of inertia of a grain i with radius r_i and mass m_i is given by $J_i = J^* m_i R_i^2/2$. A simulation with $J^* = 1$ corresponds to the realistic situation of the grains' rotation. By varying J^*, one can investigate situations where the rotation is either enhanced ($J^* \ll 1$) or is hindered ($J^* \gg 1$).

Changing the value of J^* also impacts the quality of the segregation. As can be seen in Fig. 9, Ψ_∞ increases with J^*,

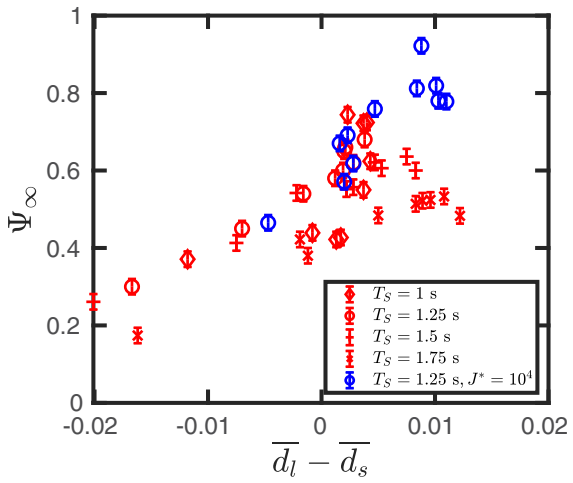

FIG. 7. Plot of the segregation quality Ψ_∞ as a function of the difference of mean displacement between the large grains and the small grains, $\overline{d_l} - \overline{d_s}$. Each tick refers to the same data set as in Fig. 6.

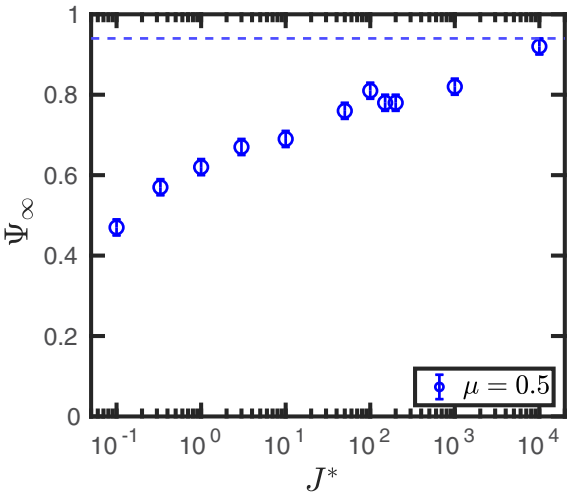

FIG. 9. Plot of the segregation quality Ψ_∞ as a function of the reduced moment of inertia J^*. The dashed line corresponds to the value of Ψ_∞ if the rotation is entirely blocked, which corresponds to $J^* \to +\infty$. The friction coefficient is the same for all the data: $\mu = 0.5$.

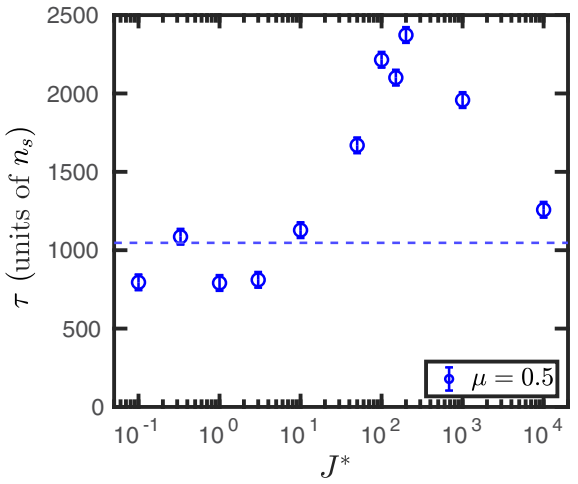

FIG. 10. Plot of the segregation time τ as a function of the reduced moment of inertia J^*. The dashed line corresponds to the value of τ if the rotation is artificially frozen, which corresponds to $J^* \to +\infty$. The friction coefficient is the same for all points: $\mu = 0.5$.

exceeding 0.9 for $J^* = 10^4$. The highest values of J^* correspond to the blue circles in Fig. 7. This monotonic evolution requires an explanation.

A good segregation quality means having wide quasi-monodisperse areas: A core of mostly small grains surrounded by a ring a mostly large grains (see Fig. 2). In these quasi-monodisperse areas, the grains tend to self-organize in a hexagonal lattice, in spite of the $\pm 20\%$ dispersity in size within both species of grains. In a hexagonal lattice of disks, the rotation of the disks is frustrated, meaning that any rotation will dissipate a large quantity of energy through solid friction. Thus, for a given amount of energy injected in a quake, quasi-monodisperse areas (with quasi-hexagonal packing) will have a much lower energetic cost if the 2D grains are not able to rotate. This will enable a much better segregation quality for the same set of perturbations.

The rotational degree of freedom also impacts the characteristic segregation time τ; see Fig. 10. From the physical value $J^* = 1$, τ first increases with increasing J^* (up to $J^* = 10^2$), after which τ decreases. The increase in the range $J^* \in [1, 10^2]$ can be well understood since the grains require longer times to rearrange as their rotational motion becomes more restricted. However, for $J^* > 10^2$, the slowing effect of J^* is dominated by the energy savings discussed above when the grains tend to form quasi-monodisperse areas. The explanation is similar to the one discussed for Ψ_∞: When frictional losses decrease, the energy injected during a quake can be more efficiently used to rearrange the grains, causing the segregation to occur more quickly.

V. CONCLUSION AND FUTURE WORK

In this paper, the segregation dynamic of a 2D asteroid submitted to regular quakes was investigated. The influence of the frictional properties of individual grains and the effect of grain rotation on the segregation time and efficiency were studied. A number of parameters were kept constant and their influence on the segregation mechanisms clearly deserve further attention. Namely, it would be interesting to vary both the size ratio of the two species (only a factor 2 was used) as well as their fraction of total surface of the asteroid (1/2 large and 1/2 small grains in our study). The study of a single large intruder in an assembly of small grains might also shed some light on the segregation mechanisms. Future work should also focus on a more realistic perturbation method. Inverted gravity was used to mimic the classical "shaken granular media" experiments but simulating tidal forces, the YORP effect, or collisions between the asteroid and small bodies should be more relevant to the astrophysical community.

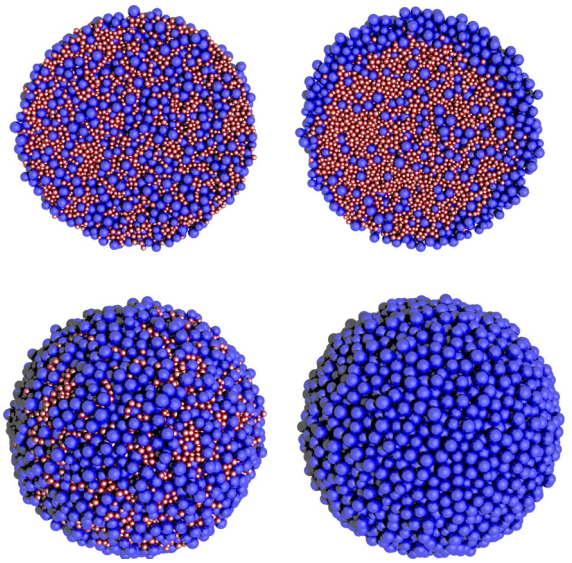

FIG. 11. Illustrations of a simulated 3D aggregate. On top: Half-cut view of the aggregate in its initial mixed state (left) and after 90 perturbations (right). Below: Outside view of the aggregate in its initial mixed state (left) and after 90 perturbations (right). The radial segregation is very clear and occurs after only a small number of quakes.

With the aim of simulating more realistic asteroids, our 2D results should be extended to 3D assemblies of grains. Preliminary simulations were performed (see Fig. 11) and show a very clear segregation. Moreover, the segregation time τ is apparently much lower than in 2D, for a comparable set of parameters. Indeed, the segregation is well advanced as early as after 50 quakes. We intuitively link this preliminary

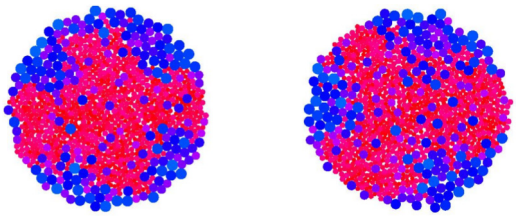

FIG. 12. Illustrations of the angular segregation in a 2D aggregate. Left: View of the asteroid after 2300 perturbations; four lobes are formed. Right: Picture of the same aggregate after 5000 perturbations, presenting only three lobes.

observation to the fact that each grain has six degrees of freedom in 3D, instead of three in 2D.

Finally, one observation in 2D asteroids clearly deserves further investigation. For some physical parameters, a secondary segregation pattern may appear. Indeed, after a clear radial segregation, the large grains eventually gather into lobes at the surface of the aggregate (see Fig. 12). This angular or orthoradial segregation displays an interesting dynamics, as the lobes may sometimes merge or split (see Fig. 12). This effect may also occur in 3D. Indeed, the half-cut view in Fig. 11 shows a clear symmetry breaking in the thickness of the layer of large grains, which can be seen as the formation of one unique lobe. These patterns are reminiscent of the surface aspect of rubble-pile asteroids, and a detailed study of this secondary segregation might shed new light on results obtained from space missions.

[1] J. Saito, H. Miyamoto, R. Nakamura, M. Ishiguro, T. Michikami, A. Nakamura, H. Demura, S. Sasaki, N. Hirata, C. Honda *et al.*, Science **312**, 1341 (2006).

[2] A. Fujiwara, J. Kawaguchi, D. Yeomans, M. Abe, T. Mukai, T. Okada, J. Saito, H. Yano, M. Yoshikawa, D. Scheeres *et al.*, Science **312**, 1330 (2006).

[3] S. R. Chesley, D. Farnocchia, M. C. Nolan, D. Vokrouhlický, P. W. Chodas, A. Milani, F. Spoto, B. Rozitis, L. A. Benner, W. F. Bottke *et al.*, Icarus **235**, 5 (2014).

[4] D. DellaGiustina, J. Emery, D. Golish, B. Rozitis, C. Bennett, K. Burke, R.-L. Ballouz, K. Becker, P. Christensen, C. D. d'Aubigny *et al.*, Nat. Astron. **3**, 341 (2019).

[5] D. Hestroffer, P. Sánchez, L. Staron, A. C. Bagatin, S. Eggl, W. Losert, N. Murdoch, E. Opsomer, F. Radjai, D. C. Richardson *et al.*, Astron. Astrophys. Rev. **27**, 6 (2019).

[6] P. Sánchez and D. J. Scheeres, Planet. Space Sci. **157**, 39 (2018).

[7] T. Shinbrot, T. Sabuwala, T. Siu, M. V. Vivar Lazo, and P. Chakraborty, Phys. Rev. Lett. **118**, 111101 (2017).

[8] W. F. Bottke, Jr, D. Vokrouhlický, D. P. Rubincam, and D. Nesvorný, Annu. Rev. Earth Planet. Sci. **34**, 157 (2006).

[9] D. Scheeres, M. Abe, M. Yoshikawa, R. Nakamura, R. Gaskell, and P. Abell, Icarus **188**, 425 (2007).

[10] C. Maurel, R.-L. Ballouz, D. C. Richardson, P. Michel, and S. R. Schwartz, Month. Not. R. Astron. Soc. **464**, 2866 (2016).

[11] V. Perera, A. P. Jackson, E. Asphaug, and R.-L. Ballouz, Icarus **278**, 194 (2016).

[12] K. Ahmad and I. Smalley, Powder Technol. **8**, 69 (1973).

[13] A.P.J. Breu, H.-M. Ensner, C. A. Kruelle, and I. Rehberg, Phys. Rev. Lett. **90**, 014302 (2003).

[14] J. B. Knight, H. M. Jaeger, and S. R. Nagel, Phys. Rev. Lett. **70**, 3728 (1993).

[15] A. Rosato, K. J. Strandburg, F. Prinz, and R. H. Swendsen, Phys. Rev. Lett. **58**, 1038 (1987).

[16] S. Aumaitre, C. A. Kruelle, and I. Rehberg, Phys. Rev. E **64**, 041305 (2001).

[17] N. Taberlet, M. Newey, P. Richard, and W. Losert, J. Stat. Mech.: Theory Exp. (2006) P07013.

[18] J. Duran, *Sables, Poudres et Grains* (Eyrolles, Paris, 1997).

[19] B. Andreotti, Y. Forterre, and O. Pouliquen, *Les Milieux Granulaires: Entre Fluide et Solide* (EDP Sciences, Les Ulis, France, 2012).

[20] P. Sánchez and D. J. Scheeres, Astrophys. J. **727**, 120 (2011).

[21] P. A. Cundall and R. D. Hart, in *Analysis and Design Methods* (Elsevier, Amsterdam, 1993), pp. 231–243.

[22] T. Michikami, A. M. Nakamura, N. Hirata, R. W. Gaskell, R. Nakamura, T. Honda, C. Honda, K. Hiraoka, J. Saito, H. Demura *et al.*, Earth Planets Space **60**, 13 (2008).

[23] T. Michikami, A. M. Nakamura, and N. Hirata, Icarus **207**, 277 (2010).

[24] T. Schwager and T. Pöschel, Gran. Mat. **9**, 465 (2007).

[25] V. Becker, T. Schwager, and T. Pöschel, Phys. Rev. E **77**, 011304 (2008).